Pattern Generation by Using Multi-Step Room-Temperature Nanoimprint Lithography

Stefan Harrer, Joel K. W. Yang, Giovanni A. Salvatore, Karl K. Berggren, Filip Ilievski, Caroline A. Ross

***Abstract*—We have demonstrated multi-step room-temperature nanoimprint lithography (RTNIL) using polystyrene (PS, average molecular weight 97 kg/mol) as the imprint polymer layer on a silicon substrate for imprinting complex patterns. Single, double, and multiple (up to 10) sequential imprint steps were performed at imprint pressures between 1 to 30 MPa in separate experiments. We also transferred the imprinted patterns from the PS layer into the silicon substrate by means of an reactive-ion etching (RIE) process. To accomplish this demonstration, we designed and built a tool that controllably and repeatedly translated and pressed a sample into a stationary mold. The demonstrated inter-step alignment accuracy of this tool ranged between 80 nm and 380 nm. These experiments revealed that polymer deformation results when nanoimprint is used to further deform a previously structured surface. The molds used in these experiments consisted of 400-nm-period diffraction gratings, as well as of rectangular structures of varying aspect ratios, ranging from 150 to 300 nm wide.**

Keywords: multi-step; nanoimprint lithography; quasi-arbitrary patterns; room-temperature

I. Introduction

In this paper we demonstrate multi-step room-temperature nanoimprint lithography into 97 kg/mol polystyrene using a new nanoimprint lithography (NIL) tool that we built. To illustrate this capability, we imprinted the letters "MIT" by using five sequential imprint steps, translating the sample a programmable distance along a single direction in between steps. Finally we transferred the imprinted patterns from the polystyrene layer into the underlying silicon substrate by means of an RIE etch.

This development can be thought of analogously to the development of the typewriter after the printing press. While a printing press can replicate large-scale molds (entire pages of books) at high rates, in the typewriter, the smallest mold unit was a single letter. But the typewriter was still of great utility in an office environment. The typewriter sacrificed throughput in return for flexibility and low cost. Similarly, by removing the difficult and slow step of custom-template manufacturing from the process, our work represents a shift in how some nanoimprint work might be performed in the future.

A variety of different forms of NIL have been demonstrated in the past: thermal NIL [1], UV-cured NIL [2], and room-temperature NIL (RTNIL) [3]-[6]. But all of these existing techniques focus on pattern replication using one, or at most two, imprint steps. To make arbitrary and complex patterns, these techniques require the pre-fabrication of a custom template using some other form of lithography (typically electron-beam lithography). Our motivation in pursuing multi-step RTNIL is to create a new pattern-generation method, able to create complex and arbitrary patterns without requiring a custom template for each new pattern. In our approach, the spatial extent of each of the starting templates is only a fraction of the extent of the desired final pattern; i.e., each template is much smaller than the final pattern. Performing multiple aligned sequential imprints at room temperature with such structures would allow one to create complex structures in a sample using simple template structures. RTNIL is the only viable approach to this challenge, because it permits the mold to be removed while the polymer pattern is incomplete, thus no curing of the film is necessary. Finally the imprinted patterns must be transferred from the imprint polymer layer into the underlying substrate. Therefore an imprint polymer has to be used that is not only capable of being imprinted by room-temperature nanoimprint lithography but also of selectively being etched with respect to its carrier substrate.

Since fabricating a custom template is one of the most expensive and time-consuming steps in conventional nanoimprint lithography, and since our approach requires only a simple template, our approach will be significantly cheaper than any conventional nanoimprint lithography technique. Template fabrication by using multi-step RTNIL allows for patterning a custom template for massively parallel lithography. One can use multi-step RTNIL to fabricate custom templates for step-and-repeat fabrication processes where the use of custom templates speeds up the process of printing out large-area patterns. Multi-step RTNIL can therefore be used as

Manuscript received August 31, 2006. Manuscript revised August 30, 2007

This work was supported in part by AFOSR and the Karl Chang Innovation Fund at MIT.

S. Harrer is with the Research Laboratory of Electronics, Massachusetts Institute of Technology, Cambridge, MA 02139 USA and the Institute of Nanoelectronics at Technische Universität München, Munich, 80333 Germany (e-mail: sharrer@mit.edu)

J. K. W. Yang is with the Research Laboratory of Electronics, Massachusetts Institute of Technology, Cambridge, MA 02139 USA (e-mail: ykwjoel@mit.edu)

G. A. Salvatore is with the Research Laboratory of Electronics, Massachusetts Institute of Technology, Cambridge, MA 02139 USA and the III Facolta' at Politecnico di Turino (e-mail: salvatorega1982@yahoo.it)

K. K. Berggren is with the Research Laboratory of Electronics, Massachusetts Institute of Technology, Cambridge, MA 02139 USA (phone: 617-324-0272; fax: 617-253-8509; e-mail: berggren@mit.edu)

F. Ilievski is with the Department of Materials Science and Engineering, Massachusetts Institute of Technology, Cambridge, MA 02139 USA (e-mail: filip@mit.edu)

C. A. Ross is with the Department of Materials Science and Engineering, Massachusetts Institute of Technology, Cambridge, MA 02139 USA (e-mail: caross@mit.edu)

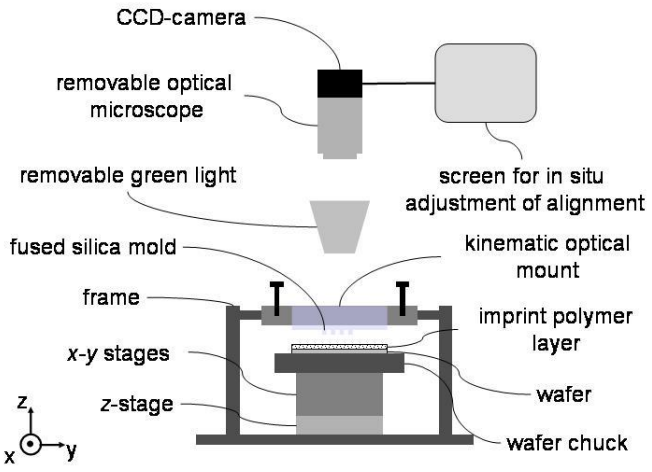

Fig. 1. Custom-built nanoimprint-lithography system used to develop our multi-step room-temperature nanoimprint method. The 3 axis-wafer stage was equipped with motor actuators having micrometer resolution and piezoactuators having nanometer resolution enabling the stage to perform three dimensional movements with nanometer precision. During the imprint process the coherent light source was replaced by an optical microscope enabling in situ compensation for misalignment.

a low-cost and time-saving technique to built arbitrary high-resolution tools for other fabrication processes.

In section II we present the details of our custom-built NIL tool. Experimental results with one- and two-step imprints are presented in section III and IV. In section V, we show proof-of-concept results of our tool. In section VI we present experimental results of the pattern transfer process from the imprint polymer layer into the substrate. Finally, in section VII we conclude with a discussion and summary of key results and future plans.

II. Description of Multi-Step Room-Temperature Nanoimprint Lithography Tool

We have designed and built a nanoimprint lithography tool that is capable of performing multi-step RTNIL cycles. In our best results, the alignment accuracy between ten sequential imprint steps was 80 nm. More typically, alignment to ± 400 nm was readily achievable.

The schematic diagram of the NIL tool is shown in Fig. 1. The tool consists of a sample chuck mounted to a linear *x*, *y*, *z* translation stage that was driven by computer-controlled stepper motors (Physik Instrumente). The mold was placed in a Newport kinematic optical mount that was affixed to a rigid frame. The core unit of the mold was a fused silica plate. We used two types of molds: (1) silicon molds with the mold patterns etched into the silicon surface, and (2) fused silica molds with the mold patterns etched into the fused silica surface. The silicon molds were glued onto a fused silica plate that was in turn mounted in the optical mount. Gluing a silicon mold onto a fused silica plate was done according to the following procedure: (1) a glue layer was manually applied to the backside of the silicon mold, (2) the silicon mold was then put upside down on a sample substrate placed on the stage so that the glue layer was facing towards the optical mount, (3) a fused silica plate was mounted in the optical mount, (4) the *z*-stage was driven upwards so that the glue layer was pressed against the fused silica plate, (5) after the glue was hardened in that position we moved the *z*-stage downwards separating mold and sample substrate. This procedure enables optimum alignment accuracy between mold and imprint substrate since the glue can still be deformed when the mold is pressed against the fused silica plate in step (4). The glue layer therefore acts as self-adjusting layer leveling out the surface planes of mold, fused silica plate, and stage. The fused silica molds were directly mounted in the optical mount. The fabrication processes for these two types of molds are described in sections III and V respectively.

A green light source was used to observe optical fringes between the bottom surface of the fused silica mold and the top surface of the substrate. The fringes were used to determine the variation in spacing between two surfaces. These surfaces were aligned to be parallel by adjusting the tilt of the mold to reduce the number of optical fringes before bringing the two surfaces into hard contact. It was crucial in our setup to ensure that both surfaces were nearly perfectly levelled in order to avoid shear forces during imprint which otherwise reduced alignment accuracy.

During the multi-step imprint procedure we used an optical microscope with a long-working-distance objective to image imprinted structures in the polymer surface by focusing through the transparent mold. The microscope was connected to a charged-coupled device (CCD) camera and a display. This setup allowed us to ensure that misalignment between imprints was less than 380 nm. The maximum area that can be imprinted on our tool is determined by the maximum scan range of the *x*, *y* stages which is a square comprising a sidelength of ~ 20 mm.

III. One-Step Room-Temperature Nanoimprint Lithography

As a first step towards performing multi-step RTNIL cycles we investigated patterns formed in a single imprint step.

One single-step RTNIL experiment consisted of the following elements: 1) spinning an imprint polymer onto a silicon wafer and baking it, 2) pressing a mold against the imprint polymer layer and imprinting it, and 3) releasing the mold from the imprint polymer layer and imaging the imprinted patterns. The main purpose of these experiments was to determine and optimize the RTNIL parameters, including imprint pressure and maximum imprint depth, when polystyrene (PS) with an average molecular weight of 97 kg/mol was used as the imprint polymer (purchased from H.W. Sands Corp.).

The maximum imprint depth depended on the depth of the mold features, the imprint pressure, the imprint duration, i.e. the period of time that the mold was in physical contact with the imprint polymer layer, as well as on the overall surface area

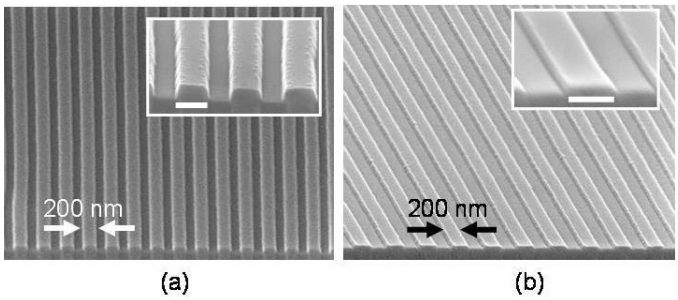

Fig. 2. (a) Scanning electron micrograph (SEM) image of the imprinted grating structure in PS after 1-step RTNIL showing 100-nm-deep grooves. The grooves of the corresponding mold were 125 nm deep. (b) SEM image of structures imprinted into PS using a 40-nm-deep grating. The imprinted grooves are 30 nm deep. Insets show a magnified view of the same grating structures. The scale bars in the insets represent 200 nm.

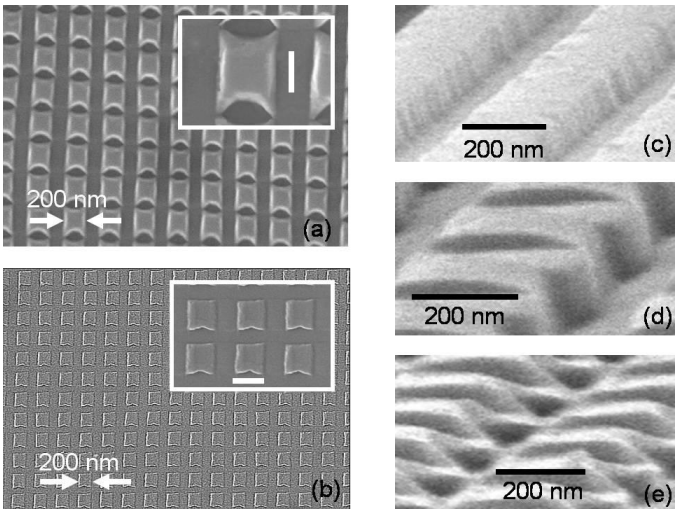

Fig. 3. (a) SEM image showing the result of two-step RTNIL with 100-nm-deep gratings. In the second imprint, the gratings were along the vertical direction. Inset shows polymer deformation/spread caused by the second imprint creating the curved edges. (b) SEM image showing the result of two-step RTNIL with 30-nm-deep grooves. With the shallower grating structure the polymer deformation caused by the second imprint was less obvious. The scale bars in the insets represent a length of 200 nm. (c)-(e) SEM images showing three phases of the evolution of the polymer deformation during the second imprint step: (c) initial state of imprinted line features after completing the first RTNIL imprint step, (b) the same line features after being deformed by an incomplete second imprint step with the grating lines of the mold being perpendicular with respect to the line features imprinted in the first imprint step, and (c) the same line features further deformed after continuing the second imprint step. Stressing out of polymer material at the edges of imprinted lines into imprinted grooves forming the eye-shaped structures as shown in (a) and (b) can be observed.

of the imprinted pattern. In order to analyze this dependency and to determine the maximum imprint depths for different depths of corresponding mold features, each single-step RTNIL experiment was performed twice using nominally identical imprint polymer layers. First a silicon mold with a 400-nm-period grating structure etched to a depth of 40 nm into the silicon was used to imprint the first imprint polymer layer. Then a mold with a 400-nm-period grating structure etched to a depth of 125 nm into silicon was used to imprint the second imprint polymer layer.

Both types of molds were fabricated using a combination of interference lithography and reactive-ion etching (RIE). A tri-layer resist process [7] was used to minimize surface reflections. The tri-layer resist consisted of 200 nm Sumitomo PFI-88 positive photoresist / 40 nm evaporated SiO_2 / 400 nm AZ Clariant BARLi-0.25 Anti-Reflective Coating. After exposure and wet development, three RIE steps were used to transfer the resist pattern into the silicon substrate: first CF_4 RIE was used to transfer the pattern into the silica interlayer, next O_2 RIE was used to etch the ARC and finally CF_4 RIE was used to etch the silicon substrate. Remaining organic residues were removed by a 15 minute immersion in H_2O:H_2O_2:NH_4OH solution in ratio 5:1:1 at 80°C. To avoid adhesion of the imprinted polymer to the mold, the surface was fluorinated by vapor deposition of tridecafluoro 1,1,2,2 tetrahydrooctyl thichlorosilane [8] (CF_3-$(CF_2)_5$-CH_2-CH_2-$SiCl_3$ from Gelest, Inc.).

The imprint polymer layer that we imprinted into consisted of Polystyrene that was first dissolved in toluene to a concentration of 5% by weight. We then spin-coated the PS/Toluene solution onto a silicon wafer at 2500 rpm and baked it at 120°C for 2 minutes resulting in a 330-nm-thick PS layer.

We used the tool described in section II to perform one imprint step at room-temperature under atmospheric conditions by applying an imprint pressure of ~30 MPa. This imprint pressure was achieved by driving the *z*-stage into the mold surface and tightening the set-screws on the optical mount. We used a strain gauge sensor mounted between stage and optical mount to measure the force with which the stage was pressed against the optical mount during an imprint step. We then calculated the imprint pressure using the known imprint area. Both types of molds were released from the imprint polymer layer after 10 s as this imprint duration proved to be the minimum period of time after which the maximum imprint depth could be achieved for both cases: the maximum imprint depth was 100 nm for the 125-nm-deep mold, and 30 nm for the 40-nm-deep mold. The imprint results presented in Fig. 2 show good sidewall and surface characteristics.

IV. Two-Step Room-Temperature Nanoimprint Lithography

As a second step towards enabling multi-step RTNIL cycles we used the same mold to perform two-step RTNIL cycles. We conducted two subsequent imprint steps onto the same area of the same imprint polymer layer with the same mold. We rotated the mold by 90° between the two imprint steps. Analogously to the described single-step RTNIL experiments, we conducted each two-step RTNIL experiment twice using nominally identical imprint polymer layers for each experiment as well as two types of molds comprising different feature depths. Fig. 3 shows the results that we obtained from using the same molds, materials, and imprint parameters as were used in the one-step RTNIL results shown in Fig. 2. During the first

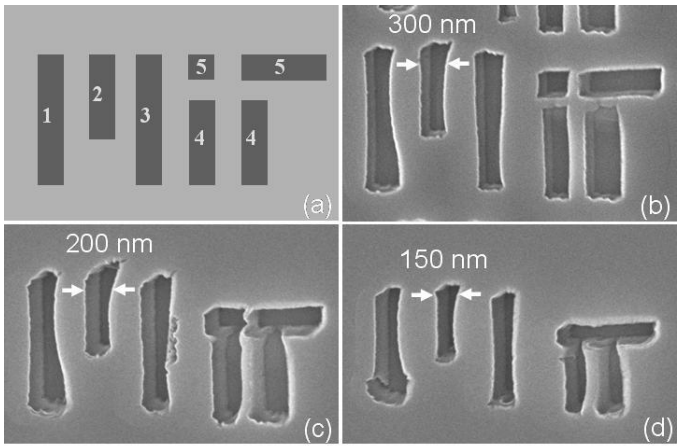

Fig. 4. Results of a 5-step RTNIL imprint cycle for different mold dimensions: (a) graphical representation of desired final pattern to be printed out. The numbers indicate the order in which parts of the final pattern were imprinted. After the 5th imprint step the pattern was complete. We performed several 5-step RTNIL cycles using molds with different feature sizes: The linewidth of the imprinted pattern in (b) is 300nm, the linewidth in (c) is 200 nm, and in (d) is 150 nm. The observed vertical and horizontal misalignment was between 80 nm and 380 nm.

imprint step the grating lines on the mold pointed in horizontal direction. The two-step RTNIL results for the mold with deeper grooves show that features that were imprinted during the first imprint step were symmetrically deformed during the second imprint step: imprint polymer was partly pressed into grooves that were imprinted during the first imprint step, forming the eye-shaped structures shown in Fig. 3a. This deformation could be significantly reduced by using a mold with less deep features as shown in Fig. 3b. When a 40-nm-deep template was used instead of a 125-nm-deep template, the structure of the imprinted features after the second imprint step became more rectangular. Fig. 3c-e illustrate the evolution of the polymer deformation leading to the eye-shaped deformation.

V. Multi-Step Room-Temperature Nanoimprint Lithography

In this section, we will describe a multi-step imprint process for imprinting a complex pattern (in this case, the MIT logo, see Fig. 4a). We fabricated a mold consisting of a variety of rectangular shapes, arrayed across the template in a pattern designed specifically for imprinting the logo, such that a total of five imprint steps were required. The order in which the imprints were made to create the final result is also shown in Fig. 4a. Structures on the mold consisted of the six rectangles and one square that make up the pattern; with the elements of each imprint step vertically displaced from the other by a distance of 2.5 μm. To form one complete pattern, we therefore needed to translate the sample along the *y*-axis by 2.5 μm in between the five imprint steps.

The mold was fabricated using 30 keV electron-beam lithography to define the rectangular structures in 950 kg/mol polymethyl - methacrylate (PMMA) spun to a thickness of

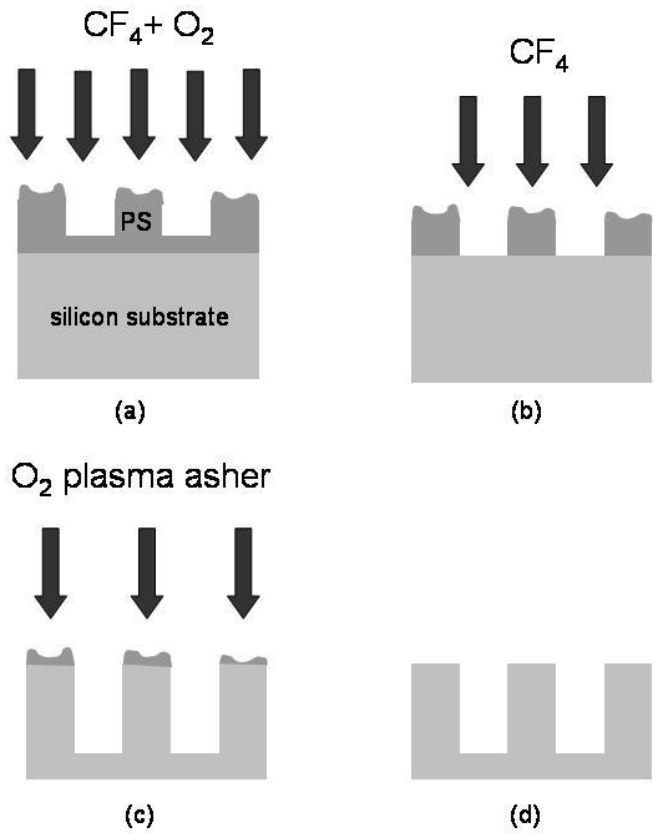

Fig. 5. Pattern transfer process: in a first step (a) the imprinted and coated sample is treated with a combined CF_4 and O_2 RIE removing the coating layer as well as residual PS from the bottom of imprinted grooves. Note that the polymer material has deformations close to the edges of imprinted grooves where polymer was pushed to the side during imprint (Fig. 4b-d). In a second step (b) CF_4 RIE was used to etch the imprinted pattern into the silicon substrate. In a third step (c) these residual deformed PS structures were stripped off by means of an O_2 plasma asher completing the transfer of the imprinted pattern from the PS layer into the silicon substrate (d).

150 nm onto a 3.81 cm diameter fused silica parallel window from CVI Laser (PW1-1525-UV). A thin layer of conductive film (Mitsubishi Aquasave) was spin-coated onto PMMA to prevent charging during electron-beam lithography. The sample was developed in 3:1 isopropyl alcohol:methyl iso-butyl ketone for 60 s. Then 40 nm of chrome was deposited onto the sample using electron-beam evaporation and patterned by using liftoff. With chrome as the etch mask, the mold structures were etched into the substrate to a depth of 270 nm by CF_4 RIE.

The sample was a silicon wafer spin-coated with 330 nm of PS. This wafer was then loaded onto our tool and held in place by concentric vacuum rings on the chuck. Mold and wafer surfaces were then leveled before the imprint cycle.

Imprints were performed by driving the *z*-stage to a stop into the mold. As the total area that was imprinted into PS was small (~ $(3.5\ \text{mm})^2$), the force applied by driving the *z*-stage into the mold was sufficient to imprint the rectangular

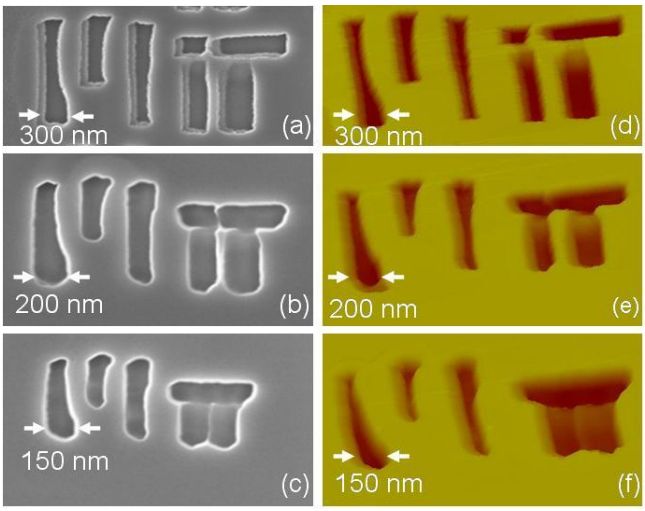

Fig. 6. SEM and AFM images of etched patterns shown in Fig. 4b-d: SEM images of (a) a 300 nm linewidth pattern after being transferred into the silicon substrate, (b) a transferred 200 nm linewidth pattern, and (c) a 150 nm linewidth pattern. Fig. 6d-f are AFM images of the exact same features as shown in Fig. 6a-c. PS was completely removed by means of an O_2 plasma asher. Throughout the pattern-transfer-etching process, features were partly merging because the corresponding imprinted PS features were deformed during the multi-step room-temperature nanoimprint process and therefore not perfectly separated from each other before the pattern transfer. SEM images were taken at a slight angle revealing the sidewalls of transferred trenches.

structures without having to tighten the set screws on the optical mount as done in section III and IV.

In our best results, a total of ten imprint steps were performed that resulted in six completed MIT logos. Fig. 4b, c, d show the imprinted result of MIT logos of different sizes. The patterns are obviously distorted. In contrast, isolated features (which were not in the proximity of subsequently imprinted features) did not show evidence of distortion.

VI. Patttern Transfer into the Silicon substrate

The multi-step room-temperature nanoimprint lithography procedure was completed by transferring the imprinted patterns from the PS layer into the silicon substrate. At the start of this step the wafer had a 5-nm-thick residual Au/Pd layer, used to alleviate charging during SEM imaging. First we performed a combined CF_4 and O_2 RIE for 4 min to etch down the PS layer everywhere until all residual PS was removed from the bottom areas of the imprinted grooves (Fig. 5a/b). In order to prevent the imprint polymer from heating up and losing its imprinted shape during the RIE process, we split this etching step into two subsequent 2-min-long etching steps that also removed the ~5 nm thick Au/Pd coating. The multi-step room-temperature process is a volume preserving patterning process, thus causing imprint polymer material to be pushed away from mold features and forming raised deformations at the edges of imprinted features with an average height of 40 nm. These deformations must not be transferred into the silicon. Therefore we stopped the CF_4 RIE before the remaining PS layer in the non-imprinted region had cleared after three subsequent 2-min-long steps (Fig. 5b/c). The etch rate of the CF_4/O_2 RIE for PS was ~ 40 nm/min and the etch rate of CF_4 for silicon was ~ 25 nm/min. We could etch the transfer pattern ~ 100-nm into the silicon layer. Finally the deformed residual PS patterns were stripped off in an O_2 plasma asher for 5 min (Fig. 5c/d).

Figures 6a-c show experimental results for the described pattern transfer process for the exact same structures as shown in Figures 4b-d. All PS material had been stripped off, so the images show silicon surfaces. Fig. 6 shows that local surface roughness of the PS layer and deformations at the edges of imprinted PS features were eliminated throughout the RIE steps.

VII. Discussion and Summary

Before this technique can be used as it is ultimately intended, as a method for the generation of complex patterns across a wide variety of length scales using only a simple set of generic template structures, at least three key issues must be addressed: (1) the mold and substrate alignment after arbitrary translations must be demonstrated (in the current work, translations were made monotonically along the *y*-axis in sequential imprints); (2) the distortion effect must be understood and controlled (we believe the observed distortion could be reduced by working with a thinner resist layer); and (3) the ability to perform overlapping imprints and thus to create extended features (such as wires) must be demonstrated. Additionally the pattern-transfer process has to be improved to allow control of the depth of the features etched into the silicon substrate independent of the thickness of the imprint polymer layer. One could perhaps address that issue by including a SiO_2 layer between the silicon substrate and the imprint polymer layer that acts as a hard etch mask for CF_4 RIE.

Nonetheless, the work provides a key demonstration that RTNIL is a useful pattern-generation tool. By building a custom tool, and by using low density polystyrene (97 kg/mol) and small-area molds, we were able to create a complex non-regular pattern out of a set of aligned sequential imprints. Using this setup, we also performed one- and two-step RTNIL using a mold with a 400-nm-pitch grating. We further developed a pattern-transfer procedure that allowed transfer of the imprinted patterns from the PS layer into the silicon substrate. Future work will focus on improving the alignment capabilities, understanding and correcting the observed image distortion of imprinted patterns as well as of etched transfer patterns, and creating increasingly complex, high-resolution, and useful structures.

Acknowledgment

We would like to thank Prof. Henry I. Smith, Prof. Minghao Qi, Dr. Euclid Moon, Dr. Timothy A. Savas, James Daley, Dr. Ion Bita, and Ozge A. Halatci for technical assistance and discussion. We would like to thank Prof. Dr. Paolo Lugli for his kind cooperation. We would also like to thank the Bund der Freunde der Technischen Universität München for supporting part of our work. This work made use of MIT's shared scanning-electron-beam-lithography facility in

the Research Laboratory of Electronics (SEBL at RLE). The authors gratefully acknowledge the financial support of AFOSR and the Karl Chang Innovation Fund at MIT. Special thanks to Jaye Jillson from PI (Physik Instrumente) L.P. for supporting the final assembly of our imprint tool. This work was supported in part by the MRSEC Program of the National Science Foundation under award number DMR 02-13282.

REFERENCES

[1] S. Y. Chou, P. R. Krauss, and P. J. Renstrom, "Imprint lithography with 25-nanometer resolution," Science, vol. 272, pp. 85-87, 1996.

[2] M. Colburn, S. Johnson, M. Stewart, S. Damle, T. Bailey, B. Choi, M. Wedlake, T. Michaelson, S. V. Sreenivasan, J. Ekerdt, and C. G. Willson, "Step and flash imprint lithography: a new approach to high-resolution patterning," SPIE Conference on Emerging Lithographic Technologies III, vol. 3676, pp. 379-389, 1999.

[3] D.-Y. Khang, H. Yoon, and H. H. Lee, "Room-temperature imprint lithography," Adv. Mater., vol. 13, pp. 749-752, 2001.

[4] D. Pisignano, L. Persano, P. Visconti, R. Cingolani, G. Gigli, G. Barbarella, and L. Favaretto, "Oligomer-based organic distributed feedback lasers by room-temperature nanoimprint lithography," Appl. Phys. Lett., vol. 83, pp. 2545-2547, 2003.

[5] E. Mele, D. Pisignano, M. Mazzeo, L. Persano, and G. Gigli, "Room-temperature nanoimprinting on metallo-organic complexes," J. Vac.Sci. Technol. B, vol. 22, pp. 981-984, 2004.

[6] E. Mele, F. Di Benedetto, L. Persano, R. Cingolani, and D. Pisignano, "Multilevel, room-temperature nanoimprint lithography for conjugated polymer-based photonics," Nano Letters, vol. 5, pp. 1915-1919, 2005.

[7] M. L. Schattenburg, R. J. Aucoin, and R. C. Fleming, "Optically matched trilevel resist process for nanostructure fabrication," J. Vac. Sci. Technol. B., vol. 13, pp. 3007-3011, 1995.

[8] T. M. Mayer, M. P. de Boer, N. D. Shinn, P. J. Clews, and T. A. Michalske, "Chemical vapor deposition of fluoroalkylsilane monolayer films for adhesion control in microelectromechanical systems," J. Vac. Sci. Technol. B, vol. 18, pp. 2433-2440, 2000.

Stefan Harrer received a BSc degree in EECS (2003) and a Diploma in EECS (2004) from the Technical University of Munich, Germany, and is now working towards his PhD degree at the Institute for Nanoelectronics at the Technical University of Munich. He also studied Technology Management at the Center for Digital Technology and Management of the Ludwig-Maximilians Universität München, the Technical University of Munich and UC Berkeley and received an Hon. Masters Certificate in Technology Management in 2003.

He was a visiting graduate student in the MIT Department of Electrical Engineering and Computer Science in 2005 and 2006 where he worked on implementing new nanoimprint-lithography techniques. He has authored and coauthored several technical publications, and has two patents pending. His research interests include nanofabrication technologies with special focus on nanoimprint lithography.

Mr. Harrer was awarded the IEEE Best Student Paper Award on the 6th IEEE International Conference on Nanotechnology 2006, Cincinnati, USA.

Joel K. W. Yang is currently a graduate student in the MIT Department of Electrical Engineering and Computer Science. He received his BSc degree in EECS (2003) from Nanyang Technological University, Singapore, and his SM degree in EECS (2005) from MIT.

He has authored and coauthored several technical publications, and has several patents pending. His research focuses on developing nanofabrication technology for superconductive nanowire single-photon detectors. These detectors have a variety of potential applications, including interplanetary-length-scale optical communications, and VLSI circuit diagnostics.

Giovanni A. Salvatore received his BSc degree in electrical engineering from Politecnico of Turin, Italy in 2004, and the MSc degree in Micro- and Nanotechnology for the ICT from Politecnico of Turin, Italy, Ecole Polytechnique Fédérale de Lausanne (EPFL), Switzerland, and the Institut National Polytechnique de Grenoble (INPG), France in 2006.

In 2006 he joined the Laboratory of Micro and Nanoelectronics Devices (LEG2) at EPFL, Switzerland, where he is now pursuing a PhD in micro- and nano-electronic devices for memory applications. His work is focused mainly on ferroelectric devices and MEMS.

Mr. Salvatore was awarded the Accenture Best Thesis in Electronics Award 2006 at Politecnico of Turin.

Karl K. Berggren holds a B.A. (1990) and a PhD (1997) in Physics from Harvard University and is now the Emanuel E. Landsman (1958) Career Development Associate Professor of Electrical Engineering at the Massachusetts Institute of Technology, Department of Electrical Engineering and Computer Science, where he heads the Quantum Nanostructures and Nanofabrication Group. He is also codirector of the Nanostructures Laboratory in the Research Laboratory of Electronics. He is also a core faculty member in the Microsystems Technology Laboratory (MTL). From December of 1996 to September of 2003, Prof. Berggren served as a staff member at MIT Lincoln Laboratory in Lexington, Massachusetts.

His current research focuses on methods of nanofabrication, especially applied to superconductive quantum circuits, photodetectors, high-speed superconductive electronics, and energy systems. His thesis work focused on nanolithographic methods using neutral atoms.

Filip Ilievski is currently a graduate student in the MIT Department of Materials Science and Engineering. He received his BSc degree in Materials Science and Engineering from MIT in 2003.

He has coauthored several technical publications in the field of magnetic materials. His current research focuses on developing templated block copolymer lithography as a tool for patterning, a process that, among a variety of other potential applications, could also be used to fabricate patterned magnetic data storage devices.

Caroline A. Ross is a professor in the Department of Materials Science and Engineering at MIT. She obtained a PhD from Cambridge University, UK and worked as a postdoctoral fellow at Harvard and as a research engineer at Komag, Inc. in California before joining MIT.

Her research interests include magnetic thin films and devices, nanopatterning and self-assembly.